

RSC Advances

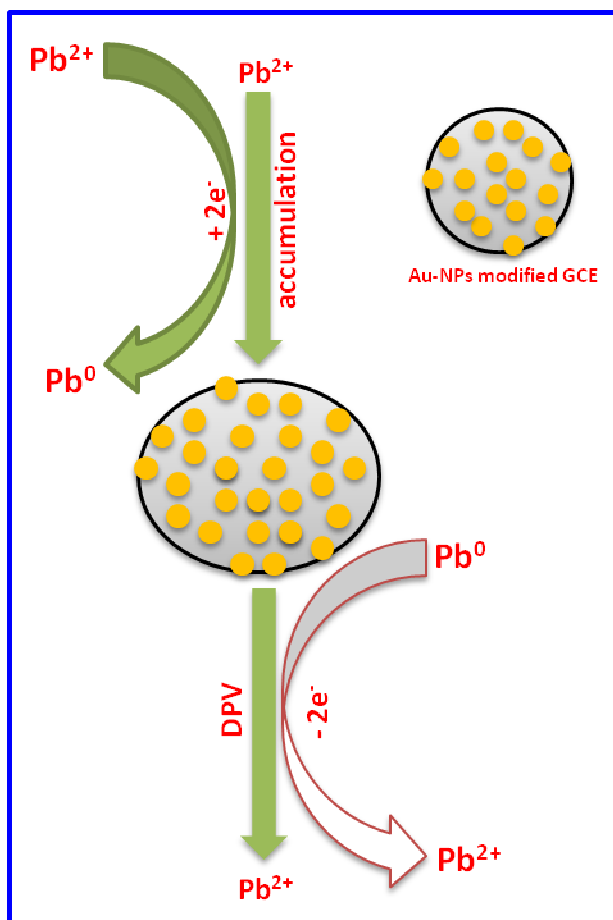


This is an *Accepted Manuscript*, which has been through the Royal Society of Chemistry peer review process and has been accepted for publication.

Accepted Manuscripts are published online shortly after acceptance, before technical editing, formatting and proof reading. Using this free service, authors can make their results available to the community, in citable form, before we publish the edited article. This *Accepted Manuscript* will be replaced by the edited, formatted and paginated article as soon as this is available.

You can find more information about *Accepted Manuscripts* in the [Information for Authors](#).

Please note that technical editing may introduce minor changes to the text and/or graphics, which may alter content. The journal's standard [Terms & Conditions](#) and the [Ethical guidelines](#) still apply. In no event shall the Royal Society of Chemistry be held responsible for any errors or omissions in this *Accepted Manuscript* or any consequences arising from the use of any information it contains.



ARTICLE

Green synthesis of gold nanoparticles and its application for trace level determination of Painter's colic

Cite this: DOI: 10.1039/x0xx00000x

Received 00th January 2012,
Accepted 00th January 2012

DOI: 10.1039/x0xx00000x

www.rsc.org/

K. Chelladurai,^a P. Selvakumar,^a S.M. Chen,^{a*} R. Emmanuel,^b K. Muthupandi,^b
P. Prakash,^{b**}

The green synthesis of metal nanoparticles is found to be more attractive in various disciplines including analytical chemistry. The present study demonstrates a selective voltammetric determination of Painter's colic (lead poisoning) using green synthesized gold nanoparticles (Au-NPs) modified glassy carbon electrode (GCE). The Au-NPs were synthesized by the reduction of chloroaurate ions with fresh leaf extract of *Justicia glauca*. The formations of Au-NPs were confirmed by UV-Visible spectroscopy using surface Plasmon resonance. The average size of the synthesized Au-NPs is found to be 32.5 ± 0.25 . A good cathodic response current is observed at Au-NPs modified electrode, while unmodified electrode does not show any response in the presence of Pb^{2+} . With optimum condition, the Au-NPs modified electrode exhibits a good response towards Pb^{2+} with the linear response range from 0.005 to $800 \mu\text{M L}^{-1}$ and lowest detection limit of 0.07 nM L^{-1} . The fabricated sensor exhibits a high selectivity towards Pb^{2+} in the presence of 100 fold concentrations of other metal ions. In addition, the proposed sensor also shows a good practicality towards Pb^{2+} in the river water samples.

1. Introduction

Lead ion (Pb^{2+}) is considered as one of the most common toxic heavy metals, which easily accumulates in plants and animals.¹ It also can cause adverse effects on human health and the environment, resulting in neurological, cardiovascular and developmental disorders, even at very low levels. Lead poisoning (also known as plumbism, colica pictorum, saturnism, Devon colic, or painter's colic) is a type of metal poisoning in humans and other vertebrates caused by increased levels of lead in the body. Lead interferes with a variety of body processes and is toxic to many

organs and tissues including the heart, bones, intestines, kidneys, and reproductive and nervous systems. It interferes with the development of the nervous system and is therefore particularly toxic to children, causing potentially permanent learning and behavior disorders.² A recent report by CDC (Centers for Disease Control and Prevention-2014) Childhood Lead Poisoning Prevention Program suggests that even a blood level of 10 micrograms per deciliter can have harmful effects on children's learning behavior. No safe threshold for lead exposure has been so far discovered—that is, there is no known sufficiently small amount of lead that will not

cause harm to the body.³ According to the US Environmental Protection Agency (EPA), the maximum contamination level for Pb^{2+} in potable water is about 75 nM L^{-1} . Hence the monitoring of Pb^{2+} below this level remains a highly challenging task.³ Over the past decades, many methods have been developed for the trace level detection of Pb^{2+} .⁴ Electrochemical detection of Pb^{2+} has been paid much attention due to its simplicity and portability compared with traditional methods such as inductively coupled plasma mass spectrometry (ICPMS), thermal ionization mass spectrometry (TIMS) and X-ray fluorescence spectrometry (XRF).⁵ Recently, many sensitive and selective Pb^{2+} sensors have been developed using different modifiers on the electrodes, such as enzymes, carbon nanomaterials, polymers, and functional nanoparticles.⁶⁻¹¹ Metal nanoparticles have found particular interest in the detection of Pb^{2+} owing to their unique electronic, magnetic, catalytic and optical properties, which are different from bulk metals and dependent on their size and shape.¹²

In particular, gold nanoparticles (Au-NPs) are one of the emerging as well as predominant metal nanoparticles, which play an important role in many research areas including heavy metal ion determination.^{13, 14} There are umpteen numbers of research works as well as manufacturing procedures, which have been put into practice for the synthesis of Au-NPs, comprising a variety of physical and chemical methods, electrochemical reduction, heat evaporation, photochemical reduction, laser ablation, inert gas condensation, thermolysis and radiolysis.^{15, 16} But the presently available physical methods result in the low production rate of Au-NPs with high expenditure.¹⁵ Also, chemical methods involve toxic chemicals that will be adsorbed on the surface of Au-NPs. Further, the large scale production of Au-NPs is unfeasible because of certain drawbacks such as polydispersity and stability. Hence, there is an increasing need to develop high-yield, low cost, non-toxic and environmentally

benign procedures for the synthesis of Au-NPs. At the moment, the implementation of an alternative option, i.e. the greener approach has become a promising method for synthesis of Au-NPs. In our previous study, we had synthesized Au-NPs using *Acacia nilotica* twig bark extract as a biomaterial.¹⁷ In the present study, an attempt has been made to synthesize Au-NPs extracellularly using *Justicia glauca* leaf extract. The species *Justicia* is one of the largest species of *Acanthaceae*, with approximately 600 species that are found in pan tropical and tropical regions as perennial herbs or sub shrubs. *Justicia glauca* mainly contains water-soluble heterocyclic compounds such as lignans, alkaloids, flavonoids, steroids and terpenoids.^{18, 19} These biomolecules in leaf extract are responsible for the reduction of chloroaurate ions. Recently, Au-NPs have been used as a modifier for the sensing of heavy metals, including green derived metal nanoparticles.^{13, 14, 20} In our earlier report, we have demonstrated the green synthesis of Au-NPs using a plant extract for the electrochemical determination of nitrobenzene.¹⁷ Nonetheless, there are no reports available in the literature for the selective electrochemical determination of Pb^{2+} using Au-NPs. To the best of our knowledge, this is the first report for the selective trace level detection of Pb^{2+} using green derived Au-NPs.

In the present study, we have demonstrated the green synthesis of Au-NPs using *Justicia glauca* leaf extract as a reducing agent. The green synthesized Au-NPs modified glassy carbon electrode (GCE) has been further used for the selective determination of Pb^{2+} . The essential parameters towards the response to Pb^{2+} , such as solution pH, accumulation potential and the accumulation time have been optimized and discussed in detail. The proposed sensor shows a good analytical performance towards Pb^{2+} and the analytical performances (limit of detection and linear response range) are more comparable with recently reported Pb^{2+} sensors (Table 1). In addition, the selectivity and practicality of the

Au-NPs modified electrode toward the determination of Pb^{2+} has also been discussed elaborately.

2. Experimental

Materials

The chloroauric acid ($\text{HAuCl}_4 \cdot 3\text{H}_2\text{O}$) was purchased from Sigma–Aldrich and used as received. The leaves of *Justicia glauca* were collected from Sirumalai hills region, Tamil Nadu, India. The supporting electrolyte pH 5 (acetate buffer) solution was prepared by using 0.05 M Na_2HPO_4 and NaH_2PO_4 solutions in doubly distilled water. All the chemicals used in this work were of analytical grade and all the solutions were prepared using doubly distilled water without any further purification.

Methods

The size and morphology of Au-NPs were examined using the Transmission electron microscopy (TEM) model on a JEOL JEM 2100 instrument. JEOL JEM 2100 instrument attached with Energy Dispersive X-ray (EDX) Analyzer was used for elemental analysis. Fourier transform infrared spectroscopy (FT-IR) measurement was carried out using the Shimadzu FTIR-8201PC instrument. Jasco V-560 double-beam spectrophotometer was used for UV–visible spectral analysis. The X-ray diffraction (XRD) spectra were recorded and analyzed for the purified Au-NPs with X-ray diffraction analysis by XPERT-PRO, PW3050/60 diffractometer. Cyclic voltammetry (CV) and differential pulse voltammetry (DPV) were employed using a computerized electrochemical workstation CHI 750a work station. A conventional three-electrode assembly consisting of a modified glassy carbon electrode (GCE) as a working electrode, an Ag/AgCl electrode (Sat. KCl) as a reference electrode and a platinum wire with 0.5 mm diameter as a counter electrode was used for electrochemical experiments.

Preparation of *Justicia glauca* leaf extract

Leaves of *Justicia glauca* were cleansed to remove adhering mud particles as well as possible impurities. Subsequently, the leaves were laid on the filter paper to eliminate any moisture content in leaves and it was air-dried at room temperature for an hour. 0.300 g leaves were weighed and cut into tiny pieces. Afterward the leaves were boiled with 300 mL of sterile distilled water in Erlenmeyer flask for 15 min and allowed to cool at room temperature. The boiled and cooled leaf extract was doubly filtered. The leaf extract was pale yellowish green in color and it was shining with fluorescent color towards sunlight.

Green synthesis of Au-NPs

For the synthesis of Au-NPs, 100 mL of aqueous solution of 1mM chloroauric acid was added to Erlenmeyer flask containing 100 mL of *Justicia glauca* leaf extract. After 10 min, the leaf extract turned to pink red indicating the formation of Au-NPs. The pink color of aqueous gold colloids became deeper and deeper and after an hour, there was no noticeable difference in the color of aqueous gold colloids. The color changes indicate the formation of Au-NPs in aqueous solution due to excitation of surface Plasmon vibration in the metal nanoparticles. Later, Au-NPs were centrifuged and washed three times with deionized water. After lyophilisation the Au-NPs were stored in a screw cap bottle for further characterization.

Fabrication of Au-NPs modified GCE

Prior to the fabrication of Au-NPs modified GCE, Au-NPs dispersion was prepared by sonicating Au-NPs (3 mg mL^{-1}) for 45 min in doubly distilled water. Then, 10 μL (optimum) of Au-NPs dispersion was drop cast onto GCE and allowed to dry at room temperature. Finally, the fabricated Au-NPs modified GCE was used for all the electrochemical experiments and it was stored at room temperature when not in use. All the electrochemical studies were

performed in pH 5 solution under N_2 atmosphere in order to avoid the diffusion of atmospheric oxygen into the electrolyte solution.

3. Results and Discussion

Characterization of synthesized Au-NPs

UV-Vis spectroscopy is one of the significant techniques to find out the formation of metal nanoparticles provided surface Plasmon resonance (SPR) exists for the metal. It was recorded from the aliquots, which was isolated from the aqueous gold colloids mixture at different time intervals of bioreduction reaction. The formation of Au-NPs was principally identified by means of change in color from pale yellowish green leaf extract to pink-red color within 10 min. The time taken for complete reduction is 1 hr. The absorption reaches constant values after 1 hr. When the stability was checked after one month, it was found that there is no change in the absorption, which indicates that the nanoparticles are stable even up to one month in ambient condition ($28^\circ C$).

Fig. S1 illustrates the UV-Vis spectra of gold colloids wherein the SPR spectral values were observed in the region 588, 562 and 542 nm at different time intervals of 10, 30 and 60 min of reaction time and it was assigned as g_1 , g_2 and g_3 respectively. The spectral result suggests that the SPR peak intensity steadily increases as a function of reaction time. Moreover, the color change arises because of the coherent oscillation of electron on the surface of nanoparticles resulting in SPR with metal nanoparticles.¹⁷ This phenomenon can only be observed in nanoparticles and it is absent in bulk material.²¹ In general, Au-NPs are known to exhibit a ruby-red color in aqueous solutions due to excitation of the surface Plasmon vibrations.²² The SPR band intensity and bandwidth are influenced by the shape of the particle, dielectric constant of the medium and temperature.²³ Therefore the interaction of light with Au-NPs leads to polarization of the free conduction electrons with respect to the much heavier ionic core of Au-NPs. Thus, an electron

dipolar oscillation is created and surface Plasmon absorption band is found. The chemically synthesized Au-NPs are homogenous in nature, spherical in shape, 40 nm in size and it exhibits the surface Plasmon band in the region of 520 nm.²⁴ Herein, the maximum absorption peak is observed in the region of 542 nm at 60 min reduction time. This peak is due to collective absorption of ruby reddish color indicating the formation of large Au-NPs. The SPR bands are used to find the dispersibility of metal nanoparticles. In colloid g_1 solution, the peak at 588 nm is characteristic of isotropic nanoparticles, where as the peak at 542 nm for g_3 solution is characteristic of Plasmon resonance of anisotropic nanoparticles.²⁵⁻²⁷

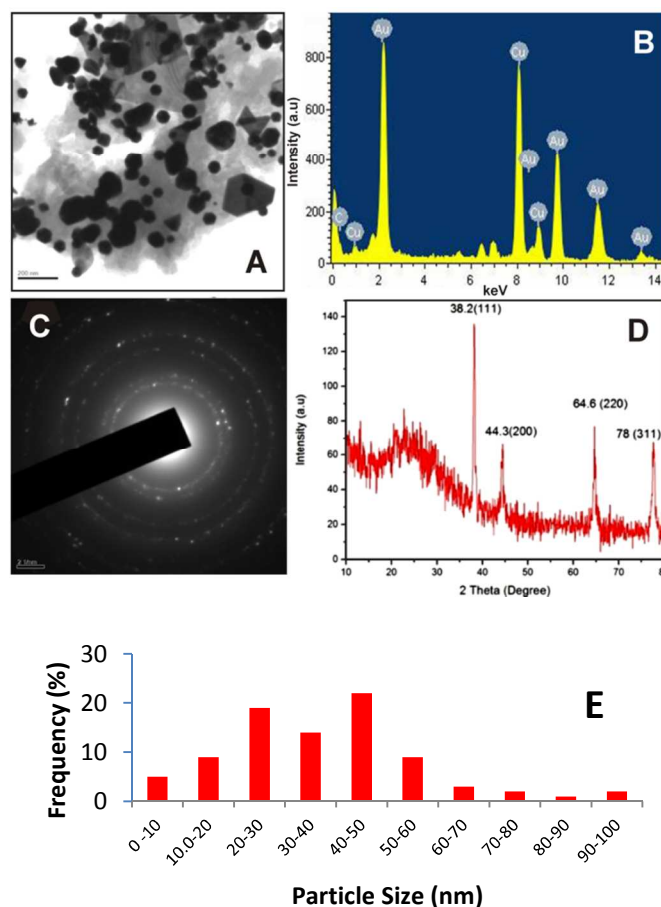


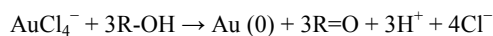
Fig. 1 (A) TEM image (scale = 100 nm and magnification = x 50 k) of green synthesized Au-NPs. Corresponding EDX (B) and SAED (C) patterns of Au-NPs. (D) X-ray diffraction patterns of Au-NPs. (E) Histogram of percent frequency distribution of Au-NPs.

Fig. 1 A shows the TEM image of green synthesized Au-NPs. The TEM images confirm that the metal particles are in nano-range, hexagonal, small number of spherical and few nanoprisms in shapes. Histogram of the percent frequency distribution of Au-NPs is shown in Fig. 1 E. The nanoprisms shaped particles have a high surface energy and it suffers a shrinking process in order to reduce the surface energy resulting in blunt-angled nanoprisms.²⁸ The EDX analysis was also used for identifying the elemental composition of gold, which indicates the kind of elements present in nanoparticles. Fig 1B illustrates that a strong signal of Au at 2 Ev confirms the formation of Au-NPs. Fig. 1C shows the SAED pattern of synthesized Au-NPs. The observation of bright circular rings correspond to (1 1 1), (2 0 0), (2 2 0) and (3 1 1) reflections of fcc gold planes, which clearly indicates that the entire nanoparticles are crystalline with the same lattice orientation running across the whole nanoparticles.²⁹

Fig. 1D shows the XRD spectrum of the purified Au-NPs. From the XRD pattern confirming with JCPDS data No. 04-0784, it can be seen that four strong diffraction peaks appear for gold at 38.2°, 44.3°, 64.6° and 78° of 2θ which correspond to (1 1 1), (2 0 0), (2 2 0) and (3 1 1) crystal planes of Au-NPs with a lattice parameter: $a = 4.078 \text{ \AA}$ and the space group, $Fm\bar{3}m$ are observed in the spectrum which agree with the Bragg's reflection of Au-NPs. There is no other significant diffraction peak detected, indicating that there is no other impurity present with Au-NPs. Furthermore, the spectra indicate a single, sharp and strong diffraction peak centered at 38.2° suggesting the strong X-ray scattering centers in the crystalline phase due to capping agents and stabilizing of nanoparticles and this can be indexed to the (1 1 1) reflection of the metallic gold with fcc structure (JCPDS File No. 04-0784). The weak diffraction peaks at 44.3°, 64.6° and 78° in the pattern agree well with the (2 0 0), (2 2 0) and (3 1 1) reflections. Generally, the

broadening of peaks in the XRD patterns of solids is attributed to the effect of particle size. Broader peaks signify smaller particle size and reflect the effects due to experimental conditions and the nucleation and growth of the crystal nuclei^{29, 30} Thus, from the XRD pattern, it can be confirmed that the products are purely Au-NPs with high crystallinity. The average size of the nanoparticles has been calculated by using Debye-Scherrer equation and it is found to be $32.5 \pm 0.25 \text{ nm}$.

The FTIR spectroscopy is a valuable tool for finding the involvement of various functional groups in the metal ion interaction during nanoparticles synthesis process. Fig. S2 shows the FTIR spectra of *Justicia glauca* leaf powder before (a) and after (b) encapsulation of Au-NPs. The band positions with corresponding functional groups are given in Table 1. The enormous variety of chemical classes has been found in the species of *Justicia*, mainly lignans, alkaloids, flavonoids, steroids and terpenoids in association with other chemical classes such as essential oils, vitamins, fatty acids and salicylic acid¹⁸⁻¹⁹. In addition, Lignans are major constituent in leaf extract and it contains phytochemical such as (+)-pinoresinol, (+)-medioresinol, (+)-lariciresinol, (+)-isolariciresinol, (+)-8-methoxy iso lariciresinol, justiciresinol and the steroids, sitosterol-3-0-glucoside, which are responsible for reduction of metal ions and efficient stabilization of nanoparticles. Hydroxyl groups (OH) are very abundant in the above all chemical constituents. In particular lignans has rich in hydroxyl groups and it could have participated in the gold reduction. These pigments have good reductive properties while AuCl_4^- is a very strong oxidizing agent and could thus aid in reduction of Au(III) to Au(0).



The above reaction indicates that reduction of Au(III) to Au(0) occurs through oxidation of hydroxyl to carbonyl groups.

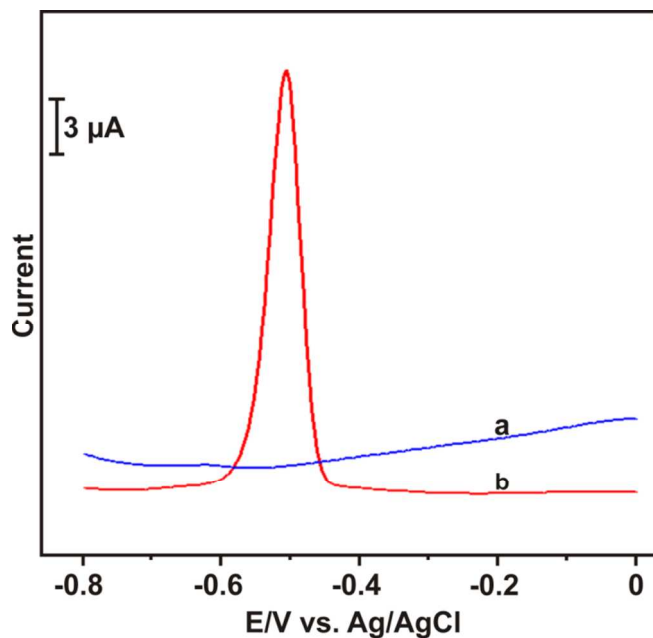
Electrochemical behavior of Pb^{2+} 

Fig. 2 Differential pulse voltammetric response of the bare (a) and Au-NPs (b) modified glassy carbon electrode response to $100 \mu\text{M L}^{-1} \text{Pb}^{2+}$ in N_2 saturated pH 5 solution.

In order to evaluate the electrochemical behavior of Pb^{2+} at different modified electrodes, the differential pulse voltammetry was performed at bare (a) and Au-NPs (b) modified electrodes in $100 \mu\text{M L}^{-1} \text{Pb}^{2+}$ containing pH 5 solution. As shown in Fig. 2, the Au-NPs modified electrode shows a well defined cathodic peak at -0.514 V , which is due to the reoxidation of Pb^0 to Pb^{2+} .⁵ With the same condition, the unmodified electrode does not show any peak response to Pb^{2+} , indicating that the bare electrode is not suitable for the determination of Pb^{2+} . The result further indicates that the good response of Pb^{2+} is derived from the presence of large active sites of Au-NPs. Hence, the Au-NPs modified electrode is more suitable for the determination of Pb^{2+} . The schematic representation for the mechanism of Pb^{2+} detection at Au-NPs modified electrode is shown in Fig. 3.

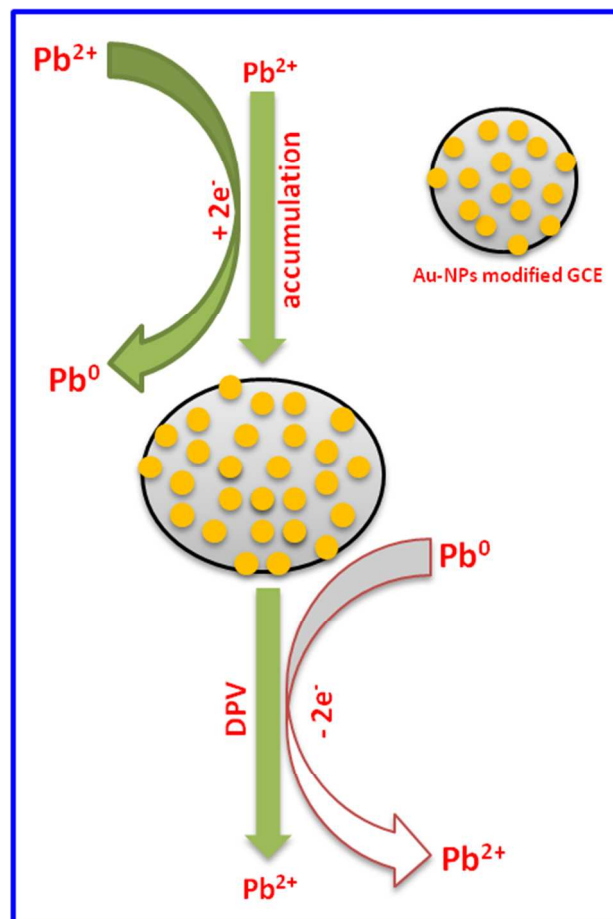


Fig. 3 Schematic representation for the detection of Pb^{2+} at Au-NPs modified electrode.

Optimization of accumulation potential and time

In order to optimize the experimental conditions to the electrochemical detection of Pb^{2+} at Au-NPs modified electrode, the effect of pH value, accumulation time and accumulation potential were studied for the response to $100 \mu\text{M L}^{-1} \text{Pb}^{2+}$ at Au-NPs modified electrode. Fig. 3 shows the effect of pH and accumulation on the DPV response of $100 \mu\text{M L}^{-1} \text{Pb}^{2+}$. A well-defined DPV response is observed in each pH solution. The response current increases gradually with the increase of pH solution from pH 2 to pH 6. An utmost current response is obtained at pH 5 solution due to low concentration of H^+ in the solution. The response current decreases when the solution pH is more than 5.0 (Fig. 3B). The current response of the modified electrode to Pb^{2+} ions decrease

below pH 5 and it may be due to the disturbance of modified electrode by the large number of hydrogen ions (H^+) in the solution. In high pH solutions (more than 7.0) the signal of Pb^{2+} starts to decrease, which may be related to the hydrolysis or valence change of the metal ions. Moreover, the pH 5 (acetate buffer) solution has been widely used as a supporting electrolyte for metal ions detection due to the low background current and good stability. Therefore, pH 5.0 was chosen as an optimum pH for further experiments.

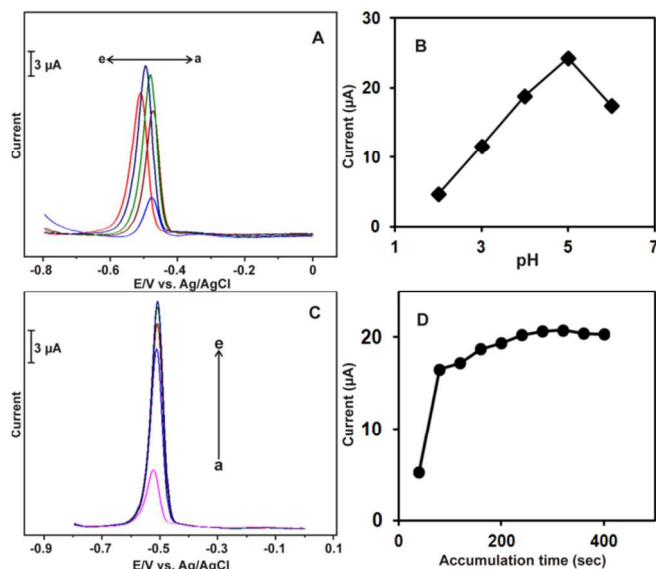


Fig. 4 A) Effect of pH on the differential pulse voltammetric response to $100 \mu M L^{-1} Pb^{2+}$ at Au-NPs modified glassy carbon electrode in pH 5 solution. B) The corresponding plot for the effect of pH vs current response. C) Differential pulse voltammetric response of the Au-NPs modified glassy carbon electrode to the response to $100 \mu M L^{-1} Pb^{2+}$ in pH 5 upon different accumulation time. D) Inset shows the corresponding plot for effect of accumulation time vs. current response.

Fig. 4C shows the effect of accumulation time on the DPV of $100 \mu M L^{-1} Pb^{2+}$ at Au-NPs modified electrode. It can be seen that the response current increases with the increase of deposition time. The utmost current response is observed at 220 s, the current response becomes saturated when the deposition time is more than 220 s. Hence the 220 s was used as an optimum accumulation time.

The effect of accumulation potential on the response to $10 \mu M Pb^{2+}$ was also studied by DPV. Fig. S2 shows the effect of different accumulation potential on the response to $100 \mu M L^{-1} Pb^{2+}$. It can be seen that the best sensitivity is observed when the deposition potential sweeps at -0.8 and -1.2 V. The current intensities of the both accumulation potential (-0.8 and -1.2 V) are identical. The current response decreases when the accumulation potential is more or less than -0.8 V. Hence, -0.8 V was chosen as an optimum accumulation potential throughout the experiments.

Determination of Pb^{2+} at Au-NPs modified electrode

The DPV was employed for the selective determination of Pb^{2+} at Au-NPs modified electrode in pH 5 solution. Fig. 4 shows the DPV response of the Au-NPs modified electrode for Pb^{2+} with different concentrations. It can be seen from Fig. 5 (inset) that the Au-NPs modified electrode exhibits a good response to each addition of $5 nM L^{-1}$, $50 nM L^{-1}$ and $1 \mu M L^{-1}$ of Pb^{2+} . The response current linearly increases with the concentration of Pb^{2+} in the range 0.005 to $800 \mu M L^{-1}$ (inset). The linear regression equation is found to be $y(\mu A) = 0.234 + 4.07x (\mu M)$ with a correlation coefficient of 0.9907. The sensitivity is calculated as $2.93 \mu A \mu M^{-1} L^{-1} cm^{-2}$ with a detection limit (DL) of $0.07 nM L^{-1}$ based on a signal-to-noise ratio of 3. In order to evaluate the analytical performance of the proposed sensor, the DL and the linear response range was compared with previously reported Pb^{2+} sensors.³⁷⁻⁴³ The comparison results are shown in Table. 2. Furthermore, the response time (6 s) of our sensor is more comparable with previously reported Pb^{2+} sensors as shown in Table. ST1. The response time of the sensor was calculated using amperometry. It has been reported early that the spherical nanoparticles have more sensitivity and selectivity than non-spherical nanoparticles due to the long stability. However, in our method most of the nanoparticles in spherical shape and this is the reason why the modified electrode has more sensitivity and

selectivity.^{44, 45} The proposed modified electrode shows a lower DL and wider linear response range toward Pb^{2+} compared to recently reported Pb^{2+} sensors.

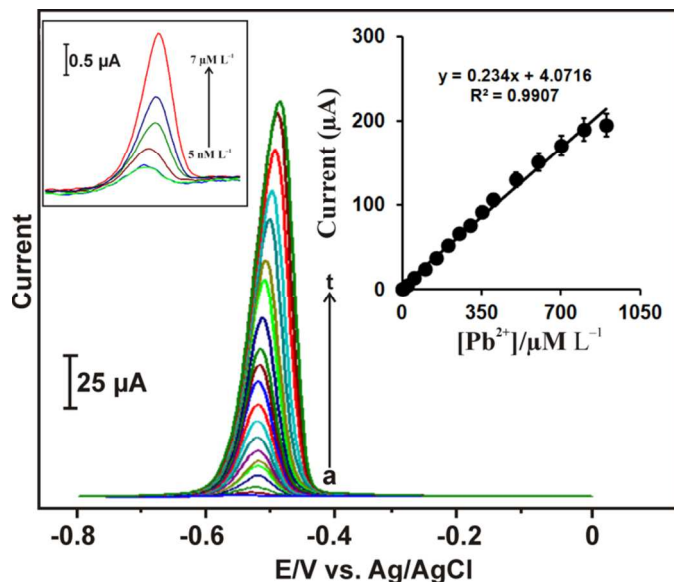


Fig. 5 Differential pulse voltammetric response of Au-NPs modified glassy carbon electrode to the different concentrations of Pb^{2+} ($0.005\text{--}900\ \mu\text{M L}^{-1}$) in pH 5 solution. Inset shows the calibration plot of current response vs. $[\text{Pb}^{2+}]$. Error bar shows the relative standard deviation of 2 measurements.

Selectivity of the sensor

In order to evaluate the selectivity of the Au-NPs modified electrode, the percentage variation of signal of $10\ \mu\text{M L}^{-1}\ \text{Pb}^{2+}$ was studied in the presence of 50 fold concentrations of metal cations by using DPV. The obtained results are summarized in Fig. 6. It can be seen from Fig. 6 that the DPV signal of $10\ \mu\text{M L}^{-1}\ \text{Pb}^{2+}$ is not affected ($< 2\%$) in the presence of Co^{3+} , Fe^{2+} , Zn^{2+} , Ca^{2+} , Mg^{2+} , Ni^{2+} and Cd^{2+} . The signal of Pb^{2+} slightly changes ($< 5\%$) in the presence of Cd^{2+} and Hg^{2+} . The Cu^{2+} shows serious effect ($< 8\%$) on the signal of Pb^{2+} at the Au-NPs modified electrode. This may be due to the formation of Pb-Cu solid solutions and similar effects have been reported previously.⁴⁶ However the effect of other metal cations including Cu^{2+} on the response of Pb^{2+} are within the acceptable limit,

hence the Au-NPs modified electrode is more suitable for the determination of Pb^{2+} .

Real sample analysis

The fabricated Au-NPs modified electrode was successfully applied to the determination of Pb^{2+} in the river water samples using standard addition method by DPV. The obtained DPV results are shown in Fig. S4A and B and the recovery results are summarized in Table 3. The proposed electrode shows good recovery results ($\sim 96\text{--}98.6\%$) towards Pb^{2+} in the river water samples, indicating a good practicality of the proposed electrode.

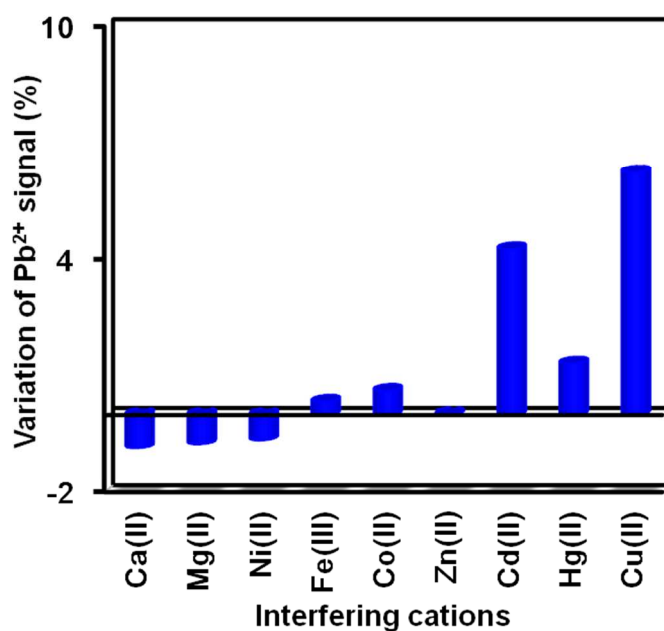


Fig. 6 The effect of 50 folds concentrations of interfering metal ions on the percentage variation of signal of $10\ \mu\text{M Pb}^{2+}$ at Au-NPs modified electrode in pH 5 solution.

Stability, repeatability and reproducibility

In order to evaluate the stability of Au-NPs modified electrode, the response of $50\ \mu\text{M L}^{-1}\ \text{Pb}^{2+}$ at Au-NPs modified electrode was examined periodically for 3 days by using DPV. The modified electrode loses the initial sensitivity about 7.4% after three days. However, no other peak potential shift is observed at the modified electrode, indicating a good stability of the Au-NPs

modified electrode. The reproducibility of the sensor was studied using 3 independently prepared Au-NPs modified electrodes towards the detection of $50 \mu\text{M L}^{-1} \text{Pb}^{2+}$ by DPV. The obtained DPV results are shown in Fig. S5. It can be seen from Fig. S5 that the 3 sensors detect the Pb^{2+} accurately with a relative standard deviation (RSD) of 2.9 %. The fabricated sensor was further employed for the detection of $50 \mu\text{M L}^{-1} \text{Pb}^{2+}$ containing 8 solutions and shows the good repeatability with a RSD of 3.6. The result indicates the good reproducibility and repeatability of the fabricated sensor.

4. Conclusions

In conclusion, a trace level determination of Pb^{2+} has been demonstrated using green synthesized Au-NPs modified electrode. The synthesized Au-NPs have been characterized by TEM, ERD, EDS and SAED analysis and the size of Au-NPs is found in the range of 15 to 55 nm. The sensitivity and LOD are calculated as $2.93 \mu\text{A} \mu\text{M}^{-1} \text{L}^{-1} \text{cm}^{-2}$ and 0.07nM L^{-1} respectively. The proposed sensor shows the high selectivity for Pb^{2+} in the presence of an excess concentration of other metal ions. Due to the good practicality of modified electrode, it can be used as a promising electrode material for the selective detection of Pb^{2+} in environmental samples.

Acknowledgments

This project was supported by the National Science Council and the Ministry of Education of Taiwan (Republic of China).

Notes and references

^aElectroanalysis and Bioelectrochemistry Lab, Department of Chemical Engineering and Biotechnology, National Taipei University of Technology, No. 1, Section 3, Chung-Hsiao East Road, Taipei 106, Taiwan, ROC. E-mail: smchen78@ms15.hinet.net;

Fax: +886-2-27025238; Tel: +886-2-27017147.

^{**}Department of Chemistry, Thiagarajar College, Madurai-625009, Tamilnadu, India.

E mail: kmpprakash@gmail.com,

Fax: +91-4522312375, Tel: +91-9842993931, +91-4522456783

1. J. Yan and E.M. Indra, *Anal. Chem.* 2012, **84**, 6122.
2. S. M. Zarcero, A. Sanchez, M. Fajardo, I.D. Hierro and I. Sierra, *Microchim Acta*, 2010, **169**, 57.
3. (<http://www.epa.gov/safewater/contaminants/index.html>).
4. N. Yildirim, F. Long, M. He, C. Gao, H.C. Shi and A.Z. Gu, *Talanta*, 2014, **129**, 617.
5. Q. Song, M. Li, L. Huang, Q. Wu, Y. Zhou and Y. Wang, *Anal. Chim. Acta*, 2013, **787**, 64.
6. C.W. Lien, Y.C. Chen and H.T.C. Huang, *Nanoscale*, 2013, **5**, 8227.
7. W. Shi, X. Zhang, S. He, and Y. Huang, *Chem. Commun.*, 2011, **47**, 10785.
8. W. Luo, Y.S. Li, J. Yuan, L. Zhu and Z. Liu, et al. *Talanta*, 2010, **81**, 901.
9. J.W. Lee, H.J. Jeon, H.J. Shin and J.K. Kang, *Chem. Commun.*, 2012, **48**, 422.
10. Y.L. Dong, H.G. Zhang, Z.U. Rahman, L. Su and X.J. Chen, et al. *Nanoscale*, 2012, **4**, 3969.
11. C.W. Lien, Y.T. Tseng, C.C. Huang and H.T. Chang, *Anal. Chem.*, 2014, **86**, 2065.
12. Kumar, S. Mandal, P.R. Selvakannan, R. Pasricha and A.B. Mandale, et al. *Langmuir*, 2003, **19**, 6277.
13. K.W. Huang, C.J. Yu and W.L. Tseng, *Biosens Bioelectron.*, 2010, **25**, 984.
14. H. Huang, S. Chen, F. Liu, Q. Zhao and B. Liao, et al. *Anal Chem*, 2013, **85**, 2312.
15. U. Kreibitz and M. Vollmer, Berlin: *Springer*, 1995.
16. Y. Li, X. Duan, Y. Qian, L. Yang and H. Liao, *J Colloid Interface Sci.*, 1999, **209**, 347.
17. R. Emmanuel, K. Chelladurai, S.M. Chen, P. Selvakumar, S. Padmavathi and P. Prakash, *J. Hazard. Mater.*, 2014, **279** 117.
18. G.M. Correa and A.F.C. Alcântara, *Brazilian Journal of Pharmacognosy*, 2012, **22**, 220.
19. N. Fukamiya and K. Lee, *J Nat Prod*, 1986, **49**, 348.
20. M. Annadhasan, T. Muthukumarasamyvel, V.R.S. Babu and N. Rajendiran, *ACS Sustainable Chem.*, Eng. 2014, **2**, 887.

ARTICLE

21. L. Lina, W. Wang, J. Huang, Q. Li and D. Sun, et al. *Chem. J.*, 2010, **162**, 852.
22. T.K. Joerger, R. Joerger, E. Olsson and G.C. Graqvist, *Proc. Natl. Acad. Sci.*, 1999, **96**, 13611.
23. T. Tanaka, S. Nagao and H. Ogawa, *Anal. Sci.*, 2001, **17**, i1081.
24. S.P. Chandran, M. Chaudhary, R. Pasricha, A. Ahmad and M. Sastry, *Biotechnol. Prog.*, 2008, **22**, 577.
25. S.L. Smitha, D. Philip and K.G. Gopchandran, *Spectrochim. Acta A*, 2009, **74**, 735.
26. N. Ahmad, S. Sharma, M.K. Alam, V.N. Singh and S.F. Shamsi, et al. *Colloids Surf., B*, 2010, **81**, 81.
27. R. Jenkins and R.L. Snyder, John Wiley and Sons, New York, 1996, 544.
28. A.N. Mishra, S. Bhadauria, M.S. Gaur, R. Pasricha and B.S. Kushwah, *Int. J. Green Nanotechnol.*, 2010, **1**, 118.
29. R. Deshpande, M.D. Bedre, S. Basavaraja, B. Sawle and S.Y. Manjunath, et al. *Colloids Surf. B*, 2010, **79**, 235.
30. Becheri, M. Durr, P.L. Nostro and P. Baglioni, *J. Nanopart Res.*, 2008, **10**, 679.
31. S.S. Shankar, A. Rai, A. Ahmad and M. Sastry, *J. Colloid Interface Sci.*, 2004, **275**, 496.
32. J.Y. Song, H.K. Jang and B.S. Kim, *Process Biochem.*, 2009, **44**, 1133.
33. R.R. Naik, S.J. Stringer, G. Agarwal, S. Jones, and M.O. Stone, *Nat. Mater.*, 2002, **1**, 169.
34. A.C. Templeton, J.J. Pietron, R.W. Murray and P. Mulvaney, *J. Phys. Chem B*, 2000, **104**, 564.
35. M.I. Husseiny, M.A. El-Aziz, Y. Badr and M.A. Mahmoud, *Spectrochim. Acta, Part A*, 2007, **67**, 1003.
36. D.C. Daniel and D. Astruc, *Chem Rev.*, 2004, **104**, 293.
37. M.O. Salles, A.P.R. Souza, J. Naozuka, P.V. Oliveira and M. Bertotti, *Electroanalysis* 2009, **21**, 1439.
38. W. Yantasee, K. Hongsirikarn, C.L. Warner, D. Choi and T. Sangvanich, et al. *Analyst* 2008, **133**, 348.
39. Bahrami, A.B. Seidani, A. Abbaspour and M. Shamsipur, *Electrochim. Acta* 2014, **118**, 92.
40. T. Alizadeh and S. Amjadi, *J. Hazard. Mater.* 2011, **190**, 451.
41. J. Guo, Y. Chai, R. Yuan, Z. Song and Z. Zou, *Sens. Actuators, B* 2011, **155**, 639.
42. Y. Wang, H. Ge, Y. Wu, G. Ye, H. Chen and X. Hu, *Talanta* 2014, **129**, 100.
43. K. Wu, S. Hu, J. Fei and W. Bai, *Anal. Chim. Acta* 2003, **129**, 215.
44. Y. Kim, R.C. Johnson and J.T. Hupp, *Nano Lett.*, 2001, **4**, 165.
45. K. Yoosaf, B.I. Ipe, C.H. Suresh, K.G. Thomas, *J. Phys. Chem. C* 2007, **111**, 12839.
46. A. Wanekaya and O.A. Sadik, *Electroanal. Chem.* 2002, **537**, 135.

Table 1. FTIR spectral data of *Justicia glauca* leaf powder before (a) and after (b) encapsulation of Au-NPs with assignment of various functional groups

| Band positions (cm ⁻¹) | | Assignment ³¹⁻³⁷ |
|------------------------------------|-----------------------|--|
| (a) | (b) | |
| 3752 and 3652 3371 | 3752 and 3652 3435 | -C- of carboxylic group hydroxyl groups |
| 2925 and 2850 1741 | 2925 and 2850 1767 | -C-H- group in aromatic ring carbonyl group as in aldehydic or ketonic group |
| 1649 | 1767 | hydroxyl groups in aromatic ring |
| 1514 | 1599 | C-C aromatic group |
| 1400 | 1425 | C-H group in aromatic ring |
| 1153 | 1153 | carbonyl group as in aldehydic or ketonic group |
| 1028 | 1018 | C-O-C of phenolic |

Table 2 Comparison of analytical performance of the proposed sensor with recently reported Pb²⁺ sensors.

| Modified electrode | LCR (μM L ⁻¹) | LOD (nM L ⁻¹) | pH | Ref. |
|--|------------------------------|------------------------------|------|-----------------|
| Bi-GME | up to 6.7 | 12.5 | 12.0 | 37 |
| DMSA-Fe ₃ O ₄ | up to 0.05 | 0.5 | 7.6 | 38 |
| IIP-CPE | up to 1.0 | 0.1 | 4.0 | 39 |
| IIP-CPE | up to 0.81 | 0.6 | 5.8 | 40 |
| L-g-MWCNTS-CPE | up to 10000 | 0.32 | 6.5 | 41 |
| NH ₂ -Cu ₃ (BTC) ₂ -GCE | up to 0.5 | 5.0 | 4.5 | 42 |
| MWCNT-GCE | up to 10 | 4.0 | 4.5 | 43 |
| Au-NPs-GCE | up to 800 | 0.07 | 5.0 | Present work |

Abbreviations:

GME – Gold microelectrode, DMSA – Dimercaptosuccinic acid, IIP – Ion imprinted polymeric nanobeads, CPE –Carbon paste electrode, L-g-MWCNTS – L-grafted Multiwalled carbon nanotubes, NH₂-Cu₃(BTC)₂ – Amino-functionalized metalorganic frameworks, GCE – Glassy carbon electrode.

Table 3 Practicality of the proposed Au-NPs modified electrode for the determination of Pb²⁺ in river water, (n=3).

| Sample | Added (μM L ⁻¹) | Found (μM L ⁻¹) | Recovery (%) | RSD (%) |
|--------|--------------------------------|--------------------------------|-----------------|---------|
| 2 | 0.5 | 0.48 | 96.0 | 4.2 |
| 3 | 1.2 | 1.19 | 99.2 | 4.7 |

Abbreviations:

RSD– Relative standard deviation of three measurements.